Sensors and Actuators for Combustion Control

A. Wachsman, S. Park, A. M. Annaswamy and A. F. Ghoniem
Department of Mechanical Engineering
Massachusetts Institute of Technology
Cambridge, MA 02139

Abstract

This paper addresses the experimental investigation of a combustion system using a backward step configuration, with the goal of understanding combustion instability and its control. In order to carry out a systematic study of the various subcomponents of the combustion dynamics including hydrodynamics and heat-release, various sensors and actuators have been included in this setup that provide new insight into the underlying mechanisms, which are discussed in this paper. A preliminary model using Proper Orthogonal Decomposition (POD) and a model-based controller using the adaptive posi-cast strategy are presented. The model and the control design are verified using an air-flow injector in the step combustor at Re=6300 and an equivalence ratio of 0.85 and are shown to result in a 7.5dB pressure reduction.

1. Introduction

Continuous combustion systems, common in power generation and propulsion applications, are susceptible to the phenomenon known as thermoacoustic instability. This instability is due to a self-sustained coupling between the acoustic field of the combustion chamber, and the heat release rate. Pressure oscillations inside the combustor cause fluctuations in the heat-release rate, which in turn produces an energy input into the acoustics, generating a feedback-loop. Under certain conditions the pressure and heat-release fluctuations are in phase, causing this feedback to be destabilizing. The resulting instability is undesirable because the large amplitude pressure and heat release rate oscillations lead to high levels of acoustic noise and vibration, as well as structural damage.

Active control of combustion dynamics is an attractive approach for achieving desired performance goals, such as reduced overall sound pressure level, reduced emissions, and increased efficiency. Typically, active combustion control has been carried out using a pressure sensor or a heat release rate sensor, and an actuator that modulates the fuel, the air, or the mixture. Early attempts often utilized a phase-delayed form of the pressure sensor signal as an input to a pulsed fuel injector, where the requisite phase delay was determined empirically [1]. More recently, model-based control has been attempted where it has been shown that an order of magnitude improvement in performance can be obtained over empirical methods [2].

A model-based control strategy is more advantageous since it is based on a quantitative description of the coupling between combustion dynamics and acoustics. This makes the problem amenable to optimization of specific performance goals. Model-based control strategy has been demonstrated successfully over the past several years. Fleifil *et al.* [3] demonstrated that an analytical combustion instability model based on flame kinematics was able to correctly predict experimentally observed unstable modes. Hathout *et al.* [4] designed a linear quadratic regulator based on this model by minimizing a cost function of unsteady pressure and control input, showing that pressure oscillations could be stabilized over a range of frequencies without energizing secondary peaks. Annaswamy *et al.* [5] validated this control design in a 1kW bench-top experimental set up to demonstrate that faster settling time and reduced control effort could be achieved. Mehta *et al.* [6] extended the flame kinematics model by incorporating the impact of exothermicity and fuel transport. In [7-9], it was shown that at high intensities, the heat-release dynamics is modeled more appropriately as a well-stirred reactor. The resulting model was shown to capture drastic changes in the stability characteristics as the operating conditions approached the lean blow-out limit [9]. The same model was shown in [10] to be stabilizable using a self-tuning controller which coped with over a 100% change in the system parameters and retained closed-loop stability.

Model-based control has also been demonstrated in combustion systems with a large convective time-delay. Using a wave-based model formulation and a general heat-release dynamics model, it has been shown that an adaptive posi-cast controller can be designed to lead to stability [11]. Its experimental implementation in a swirl-stabilized combustor was shown to result in a 30-db reduction, which was significantly larger than that with empirically designed controllers, and robust to large changes in operating conditions [12].

System identification has also been used to develop dynamic combustion models using input-output data. Brunell [13] used system identification to develop a model and model-based controller for a near full-scale combustion rig under turbulent flow conditions. Murugappan *et al*. [14] developed a system identification model and a LQG-LTR model-based controller for a 30 kW swirl stabilized spray combustor, and succeeded in reducing the overall sound pressure level 14 dB lower than an empirical (non-model-based) phase-shift controller. Neumeier *et al*. [15] developed an observer to estimate the frequencies and amplitudes of the resonant modes which were used to generate control signals. Banaszuk *et al.* [16] used an extremum-seeking algorithm to update the phase angle on-line in the phase shift controller.

Current challenges in the area of combustion control lie in two distinct directions. The first is to develop an understanding of the interactions between hydrodynamics and heat release dynamics and their impact on the underlying acoustics in the combustion system. In the cases discussed in the above references, either the flow rates were significantly low [3] or significantly high [7-9], causing the hydrodynamics to not be significant. Often, however, it has been observed in experiments [17,18] that the hydrodynamic instability does play a dominant role in the acoustic oscillations. A modeling of the interactions between these three mechanisms is therefore crucial in the control of combustors. The second challenge is to address the optimization of emissions in addition to controlling the instabilities in a combustor. In this paper, we address these two challenges by implementing a variety of sensors and actuators in a specially designed combustor that allows a parametric study of time-delay systems and their control.

The combustor that was built has a backward step feature which allows the flame to be anchored at high flow-rates, thereby leading to a more efficient combustion. There are two novel aspects to the sensors and actuators that have been included in this step combustor. One is the introduction of a *distributed* sensor array that extracts information about the spatio-temporal

fluctuations in the heat-release dynamics. In order to efficiently use this information in the control design, we employ a Proper Orthogonal Decomposition based modeling and control [19]. The second unique aspect is the introduction of air modulation at the most receptive location, which is near the step, as opposed to the more traditionally deployed fuel modulation for active control. This allows us to not only manipulate the hydrodynamic stability features in the problem but also enables us to affect the emission properties in a positive way since the addition of air makes the mixture more lean.

2. Combustor Description

The experimental test-bed is a backward-facing step combustor which provides a sudden expansion with recirculation zone that anchors the flame, as shown in Figure 1. The sensors and actuators are positioned as indicated in the figure. In the figure, p' is pressure fluctuations, $\overline{U}$ is the mean air velocity in the upstream, u_1' and u_2' are velocity fluctuations at the point of fuel injection and the step, respectively, Q' is the fluctuation in the heat release rate in the burning zone, ω' is vorticity fluctuations in the downstream from the step and A_{fuel} and A_{air} are fuel and air forcing for control.

2.1 Sensors

Pressure Sensors (S_1)

Kistler pressure sensors are used to measure the dynamic pressure response from the interior of the combustor. The 6061B thermoCOMP Quartz Pressure Sensor can measure 0-2.5 bar up to 0-250 bar.

Linear Photodiode Array (S_2)

CH* chemiluminescence is measured spatially and temporally using a new sensor design involving a linear photodiode array. An NMOS linear image sensor (S3901-128Q) is available from Hamamatsu Photonics that provides 128 individual photodiodes in a linear array. Each pixel is 2.5 mm high and 45 μm wide. A flame image can be projected onto this array using the appropriate optics, and a "linear snapshot" can be taken. This has an advantage over a single photodiode, because it provides spatial information. It also has an advantage over a CCD camera, because the data can more easily be streamed to a computer for analysis, and the amount of data can be handled in real-time for control purposes.

In the experiment, the flame image passes through an optical bandpass filter centered at 430 nm, the wavelength of CH* chemiluminescence. A bi-convex UV fused silica lens is used to focus the image of the flame onto the chip. The photodiode array has high spatial resolution in the streamwise direction, and integrates the light intensity in the vertical direction.

High Speed Camera (S_3)

To capture 2D flame images at a high resolution and high speed, a MotionPro CMOS camera from Redlake is used. The MotionPro system is designed to capture high-speed digital images and deliver them directly into a PC for analysis and documentation with maximum frame resolution of 1280 x 1024 pixels with record rates up to 1000 frames per second.

Equivalence Ratio Sensor (S_4)

The equivalence ratio sensor uses a laser and a photodetector. The laser emits a beam of light of the wavelength (3.39 μm) that is absorbed by hydrocarbons like methane and propane [20]. On the other side of the combustor, a detector is installed that is sensitive to that wavelength of light. When fuel passes through the laser beam, it absorbs some of the laser light and the detector signal is reduced. The intensity of the light can be related to fuel concentration using the Beer-Lambert law, as described by Lee *et al.* [20].

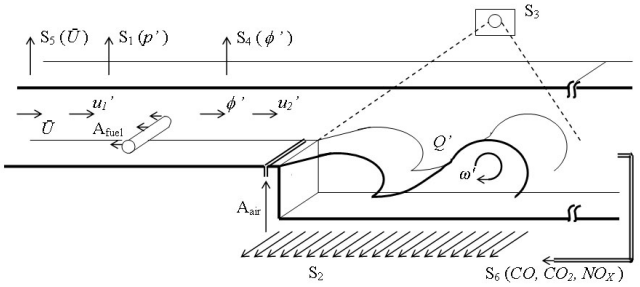

Sensors		Variables	
S_1	Pressure Sensor (p')	p'	Pressure Fluctuations
S_2	Linear Photodiode 128-array (Q')	Q'	Heat Release Fluctuations
S_3	High Speed Camera	ω '	Vorticity
S_4	Equivalence Ratio Sensor (ϕ ')	ϕ '	Equivalence Ratio Fluctuations
S_5	Air Flow Meter ($\bar{U}$)	$\bar{U}$	Mean Air Flow Rate
S_6	Emissions (CO, CO_2, NO_X)	u_1'	Velocity Perturbations at the step
Actuators		u_2'	Velocity Perturbations at the fuel bar
A_{air}	Air Forcing		
A_{fuel}	Fuel Forcing		

Figure 1 Schematic of the backward facing step combustor with various sensors and actuators

Air Flow Sensors (S_5)

The air mass flow meter is a Sierra Instruments 780S-NAA-N5-EN2-P2-V3-DD-0 Flat-Trak. The maximum flow rate is 173 *g/s*. The maximum pressure is 827 *kPa*.

Emission Sensors (S_6)

Emissions sensors are installed on the rig to provide quantitative measurements of performance characteristics such as NO_x concentration and burning efficiency. Fuel modulation is a common stabilization technique. The impact of fuel fluctuations on emissions and efficiency has been measured, but the results have not been used in the feedback loop in a way that optimizes several performance parameters simultaneously at a fixed operating condition [21,22]. Additionally, a study of emissions will provide insight into the possibility that air forcing produces cleaner emissions and more complete burning than fuel modulation. For example, air injection at the step may serve to cool the flame, reducing NO_x.

2.2 Actuators

In the following, we describe the air and fuel actuators. As indicated in Figure 2**,** the fuel injection occurs several step heights upstream pointing upstream for uniform spanwise mixing. Fuel can be modulated at an order of magnitude higher rate of the fundamental unstable frequency, but since the fuel has time to mix

in the streamwise direction before it reaches the flame, the authority of fuel modulation is reduced. Also, this type of actuation introduces a delay between the time the fuel is modulated and the time the fuel encounters the flame, which is not only moving, but also spatially distributed. Air forcing which occurs very close to the dump plane can deliver high authority for actuation energy. Also, adding additional air at the step tends to decrease the temperature, which is favorable for NO_x reduction. Detailed description of the air and fuel actuation is in the following and closed-loop control results with air actuation will be shown in Section 3.2.

Forcing Air (A_{air})

Control actuation is accomplished using a Dynamco D1B2204 Dash 1 direct solenoid poppet air valve. This valve can supply 1.8 *g/s* of air when supplied with 689 kPa. The valve is connected to a plenum beneath a 2 *mm* spanwise slot less than 1 step height upstream of the step. The break frequency of the air actuation system is 23Hz.

Fuel Forcing (A_{fuel})

Another valve used for actuation is the Moog D633-7315 AIC Direct Drive Valve (DDV). It has its own built in feedback loop to ensure the spool position using an LVDT. This feedback loop is controlled by the Moog D143-098-013 Single Axis Electronic Controller. The bandwidth of the Moog valve is 450Hz.

3. Modeling and Control of Combustion Dynamics

3.1 Modeling of the Combustion Dynamics

Figure 1 shows the various components in the backward step combustor, the locations where the underlying mechanisms may be at work, and the sensors and actuators that make up the overall combustion dynamics. Figure 2 shows the block diagram of one possible model of how these mechanisms interact with each other contributing to the overall combustion dynamics and emissions. This model illustrates the following features:

1. Two of the most dominant mechanisms that contribute to combustion dynamics are heat-release dynamics and acoustics, which are coupled through feedback.
2. Heat-release perturbations are caused by fluctuations in both the equivalence ratio (ϕ') and vorticity (ω') at the burning zone.
3. Hydrodynamics can play a dominant role in the overall dynamics if the vorticity strength, ω', is high.

Given the above features, the next step is to determine the models each of the sub-components in Figure 2. Of all the components, the acoustics is perhaps the most well understood [23]. In order to address the relative contributions of the equivalence ratio fluctuations and velocity, we have added an equivalence ratio sensor (S_4). By monitoring the corresponding fluctuations and their impact on the pressure perturbations, models of the heat-release dynamics and the inlet dynamics can be determined. In order to vary the operating conditions over a wide range and suitably monitor the conditions, we have added suitable air-flow meters (S_5). In order to assess the flame-vortex interactions so that the hydrodynamic models can be derived, we have included the linear photo-diode array (S_2). Since the spatio-temporal characteristics are likely to be the drivers here, a distributed sensor is quite necessary in this problem (S_2,S_3). While the sensor S_2 is more appropriate for real-time control, S_3 is more appropriate for flow visualization. Finally, in order to quantify the impact of active control on emissions, we have added a suite of emission sensors (S_6). At the actuators end, given that the heat-release dynamics and therefore the overall combustion dynamics is affected by two distinct types of fluctuations, due to equivalence ratio, and flame area, we have introduced two distinct actuators, A_{air} and A_{fuel}. With the above array of actuators and sensors, we expect to be able to determine the sub-component models shown in Figure 2.

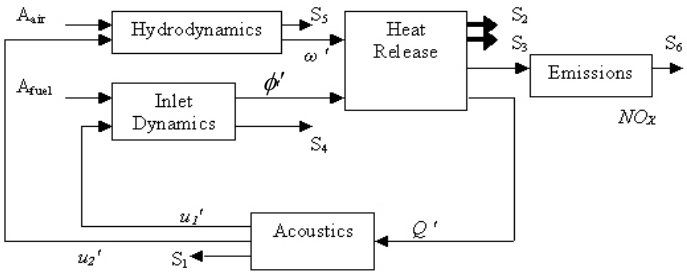

Figure 2 Schematic of acoustics, hydrodynamics and heat release dynamics interactions with different sensors and actuators.

We now present a preliminary parametric study of the impact of the inlet and hydrodynamics on combustion instability by changing operating conditions and using the sensors described in Section 2. First, fuel/air mixture inhomogeneity, ϕ', occurs due to velocity perturbations, u', at the point of fuel injection, i.e., $\phi' = \bar{\phi}/(1+\frac{u'}{\bar{U}})$. ϕ' appears at the burning zone following a convective transport time delay, τ_{tot}, determined by mean mixture velocity, $\bar{U}$, and distance from the point of fuel injection to the burning zone, L, i.e., $\tau_{tot} = L/\bar{U}$ [24]. Fluctuations in fuel/air mixture produce heat release fluctuations, Q', proportional to ϕ'. This heat variation supplies energy to acoustics exciting modal frequencies, and generating pressure and velocity fluctuations. If this feedback becomes positive, a combustion instability occurs. Second, velocity perturbations can cause repeated shedding of vortical structures, ω', at the step. This, in turn, causes the shape of the flame to change, thereby generating large amplitude of heat release fluctuation. This vortex shedding has a preferred frequency quantified by a Strouhal number $St = f_H H/\bar{U} = 0.1$ where H is the step height and f_H is the frequency (*Hz*) [25]. If the preferred vortex shedding frequency is near the acoustic mode frequency, f_{ac}, the flame is more prone to combustion instability. In the following, we describe the role of both of the above mechanisms of instability in a backward facing step combustor.

3.1.1 Role of the Inlet Dynamics (Mixture Inhomogeneity) on Combustion Instability

Obviously the convective delay from the point of fuel injection to burning zone adjusts the phase of ϕ' and thus has an impact on stability by providing positive or negative feedback. The time delay can be easily modified by changing the location of fuel injection. To determine the impact of the mixture inhomogeneity on stability, the location of the fuel injection was varied and pressure was measured at various air and fuel flow rates. Varying the location of the fuel injection further from the step has the following effects: 1) convective time delay is

increased and 2) amplitude of mixture inhomogeneity decreases due to diffusion. Note that hydrodynamic characteristics do not change by changing the location of fuel injection. We now consider two cases I and II, where the fuel bar was located 17.5*cm* and 35*cm* upstream from the step, respectively, and in both cases, the uncontrolled combustor was run at different air-flow rates. The resulting stability maps are shown in Figure 3, which illustrate the effect of varying equivalence ratio and Reynolds number. In all of the experiments, the excited acoustic mode frequency, f_{ac}, was around 38Hz. The amount of convective time delay from fuel injection point to the step, τ_{tot}, is given in the figures in terms of τ, where τ is the acoustic time scale, $1/f_{ac}$ =26.3ms. It is interesting to note that in both of the figures strong instability (over 160dB oscillations) starts to occur at $n\tau$ where n is an integer. If the instability is controlled by the mixture inhomogeneity only, a stability band should appear in the stability map depending on the time delay, i.e., unstable zones when the transport delay is between nτ and (n+0.5)τ and stable zones when the delay is between (n+0.5)τ and (n+1)τ or vice versa. This is expected due to 180 degree phase change due to time delay by switching zones. Since changes in pressure were relatively small by switching zones, it is clear that the equivalence ratio oscillation is not the dominant cause of combustion instability. However, it is still worth investigating the extent to which the mixture inhomogeneity contributes to combustion instability. Different stability characteristics shown in Figure 3 imply that the mixture inhomogeneity affects combustion instability. For this purpose, equivalence ratio oscillations (S_4) and the corresponding pressure (S_1) are compared in Case I and II at two different operating conditions. First, at Re=5300 and ϕ=0.85, as shown in Figure 4 (a), we find that in Case II, no equivalence ratio fluctuation is observed due to diffusion while in case I, equivalence ratio fluctuation is observed. Also, in Case I there is a higher pressure amplitude showing that equivalence ratio fluctuation increases pressure oscillations at this operating condition. Note that Re=5300 is in the band between (n+0.5)τ and (n+1)τ in Case I. Also, note that even without equivalence ratio fluctuations, pressure oscillations are still present in Case II. The power spectra data obtained operating at a second operating condition at Re=6300 and ϕ=0.85 is shown in Figure 4 (b). This condition corresponds to a band between nτ and (n+0.5)τ in both cases which means that equivalence ratio oscillation may damp out pressure oscillations. This is confirmed in Figure 4 (b), which shows that Case II has decreased equivalence ratio fluctuations compared to Case I while its pressure amplitude is higher. Also, note that Case I shows lower pressure oscillations in the band of τ and 1.5τ at the same Reynolds number and equivalence ratio.

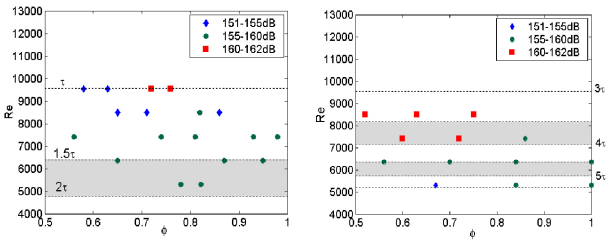

(a) Case I (fuel bar at 17.5cm) (b) Case II (fuel bar at 35 *cm*)

Figure 3 Stability maps in case I and II. Values indicate the overall sound pressure level (OASPL)

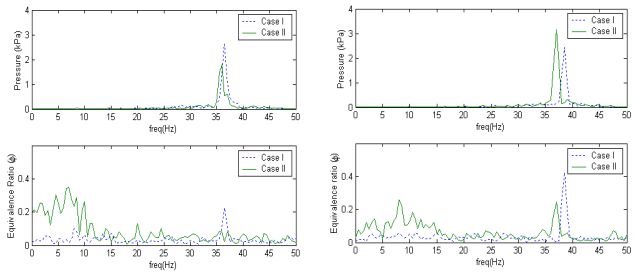

(a) Re=5300 (b)Re=6300

Figure 4 Pressure (S1) and equivalence ratio (S4) power spectra at (a) Re=5300 and ϕ=0.85 and (b) Re=6300, ϕ=0.85 in case I and case II.

3.1.2 Role of the Hydrodynamics and Flame-Vortex Interactions on Combustion Instability

The strong dependency of combustion instability on Reynolds number or mean velocity shown above suggests that the dominant mechanism causing combustion instability is hydrodynamics and its interaction with flame. As mentioned before, hydrodynamics has a preferred frequency quantified by $f_H = 0.1\overline{U}/H$. Interestingly, strong instability occurs above Re=7400 or Re=9500 which gives f_H =25Hz and 33Hz, respectively, both of which are close to the acoustic frequency, f_{ac} =38Hz. High speed CCD and linear photodiode images in Figure 5 captured at 500 frames/sec confirms strong flame–vortex interactions in Case II. In Case I, no noticeable difference in the heat release or flame structure was observed. However, these images are omitted due to space constraint. This again emphasizes that the flame-vortex interaction is the dominant mechanism of combustion instability.

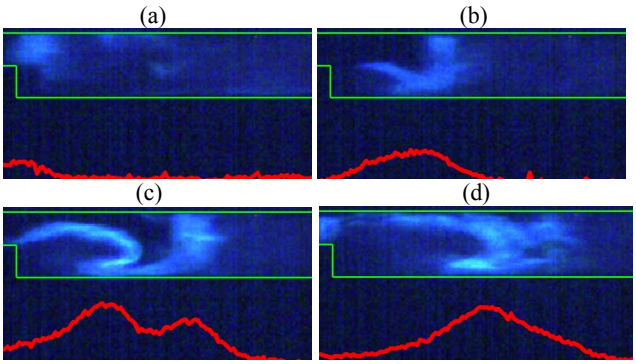

Figure 5 High speed CCD images of the flame (blue) and linear photodiode array images (red) in a backward facing step combustor (green) at Re=6300 and ϕ=0.85 in Case II. Images were taken at 500f/s. (a) p'=0 and dropping, (b) minimum p', (c) p'=0 and rising, and (d) maximum p'.

3.2 Control of Combustion Instability

Given the above results, the next step is to model the heat-release dynamics, taking into account the fact that it is strongly affected by the hydrodynamics. Since the impact of the vortices is bound to make the heat-release quite distributed, we chose the linear photodiode sensor (S_2) as the output. Since it was also observed that the hydrodynamics strongly affected the instability, we chose the air-flow modulation at the step as the actuator. The

operating condition was chosen as in Case II to be Re=6300 and ϕ=0.85. Fuel modulation in the upstream was also attempted, but its impact on combustion instability was negligible since it was not a responsible mechanism. Due to the large amount of data to be processed in closed-loop control, we use the Proper Orthogonal Decomposition (POD) method to compress spatial information in each time step [26]. POD modes are computed first using 1000 snap shots at 500 frames/sec as shown in Figure 6. The first and second modes comprise about 60% and 20% of the total energy, respectively, at the dominant acoustic frequency. Modes 3 and 4 represent harmonics of the first and the second modes.

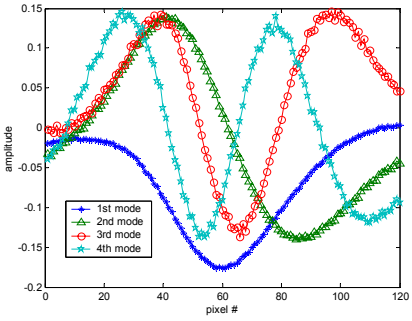

Figure 6 First 4 POD modes in a backward facing step combustor, a photodiode array with sampling rate of 500Hz was used to capture CH* intensity. 1000 snap shots are used for POD analysis.

Since the models of the sub-components shown in Figure 2 are presently not available, a System Identification model is obtained using a white noise input to the air actuator and the amplitude of the POD modes [19] as

$$G_p(s)=\frac{\alpha_1(s)}{u(s)}=G_{p,o}e^{-\tau_c s}=-\frac{s+31.8}{s^2+4.37s+5.48\times10^4}e^{-0.003s}$$

where α_1 is the amplitude of the first mode, u is the input to the control valve, $G_{p,0}$ is a delay free system, and τ_c is the time delay.

Based on the System Identification model, an adaptive posi-cast controller is designed The adaptive posi-cast controller attempts to predict future outputs using a Smith Controller, and uses a phase lead compensator to drive the future output (parameter fluctuation) to zero. The controller implemented is a discrete form, where the Smith Controller is a finite time discrete integration multiplied by a weighting function (discretized as λ_j). The weights λ_j and the gains k_1 and k_2 are adaptively updated according to the adaptation law:

$$\dot{k}(t)=-sign(k_p)\alpha_1(t)d(t-\tau),$$

where $k^T(t)=[-k_1 \quad -k_2 \quad \lambda_n(t) \quad \cdots \quad \lambda_1(t)]$, $d^T(t)=[\alpha_1 \quad u_c(t) \quad u(t-ndt) \quad \ldots \quad u(t-dt)]$, and $u_c(t)=\frac{1}{s+z_c}u(t)$. $\lambda_1 \cdots \lambda_n$ are used to eliminate the delay from the closed loop and are determined adaptively. n is determined by the time delay, τ_c, in the system ID model $G_p(s)$, $ndt=\tau_c$, where dt is the time step. k_1, k_2, and z_c are components of the phase lead compensator $k_1\frac{z_c}{s+z_c+k_2}$. z_c is selected to stabilize the unstable mode of the delay free system $G_{p,0}$, while k_1 and k_2 are determined by the adaptation law. The reader is referred to [11] for further details regarding the control design.

A schematic of the controller implementation is shown in Figure 7. The Hamamatsu linear photodiode array sends linear snapshots of the flame to the National Instruments board (PCI-6071E I/O). The NI board calculates the amplitude of the first POD mode. The amplitude is then sent to the posi-cast controller running in a dSPACE board to generate a control signal to the solenoid air forcing valve. The forcing air mass flow rate is 12% of the total air supply. In Figure 8, the closed-loop control results are illustrated, which shows that the overall sound pressure level is reduced by 7.5 dB. We note that control is turned on at $t=0$ sec

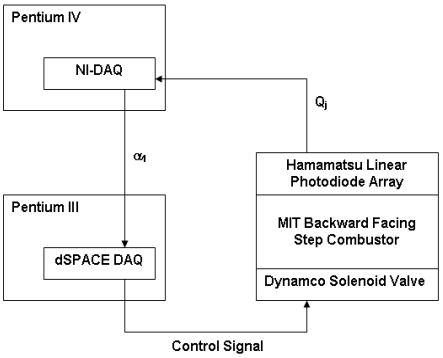

Figure 7 Control setup for POD-based adaptive posi-cast air forcing.

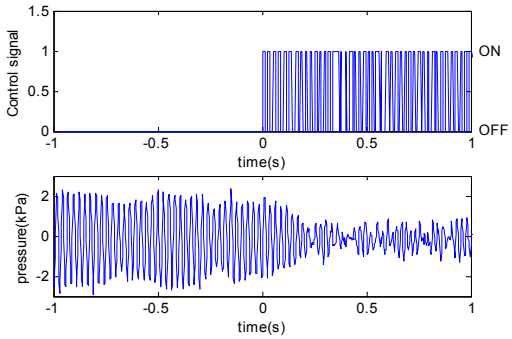

Figure 8 Pressure and control signal with and without closed-loop control. The controller was turned on at t=0 sec.

4. Summary and Concluding Remarks

In this paper, we present a variety of sensors and actuators in a specially designed combustor that allows a parametric study of time-delay systems and their control. This combustor is designed to investigate two distinct current challenges in the area of combustion control. The first is to develop an understanding of the interactions between hydrodynamics and heat release dynamics and their impact on the underlying acoustics in the combustion system which is crucial in the design of combustion control. The second is to address the optimization of emissions in addition to controlling the instabilities in a combustor.

With these sensors and actuators, a preliminary parametric study was made to investigate the impact of flame-vortex interactions and fuel/air mixture inhomogeneity on combustion instability. The location of the fuel injection is first varied which resulted in changes in the total convective time delay and magnitude of fuel/air mixture inhomogeneity. Results show that if the fuel injection is further upstream, the impact of fuel/air mixture inhomogeneity is negligible and amplitude of pressure

oscillation increase monotonically by increasing the Reynolds number. High speed CCD images of flame confirm that there is a strong flame-vortex interactions which is the dominant mechanism for combustion instability.

Finally, closed-loop control results were presented in this paper using a distributed sensor, which can capture spatio-temporal burning characteristics together with Proper Orthogonal Decomposition and an adaptive posi-cast controller. A 7.5 dB reduction in overall sound pressure level is obtained using this active control technique.

5. Acknowledgements

This work is supported by the Propulsion Program of the Office of Naval Research, grant No. N00014-99-0448, and the Defense University Research Instrumentation Program of the Army Research Office, grant No. DAAD19-01-1-0398.

References

[1] E. Gutmark, T.P. Parr, K.J. Wilson, D.M. Hanson-Parr and K.C. Shadow. "Closedloop Control in a Flame and a Dump Combustor*," IEEE Control Systems*, Vol.13, pp 73-78, April 1993.

[2] A.M. Annaswamy and A.F. Ghoniem, "Active Control of Combustion Instability: Theory and Practice," *IEEE Control Systems Magazine*, Vol. 22, No. 6, pp. 37-54, December 2002.

[3] M. Fleifil, A.M. Annaswamy, Z.A. Ghoneim, and A.F. Ghoniem, "Response of a Laminar Premixed Flame to Flow Oscillations: A Kinematic Model and Thermoacoustic Instability Results," *Combustion and Flame*, vol. 106, pp. 487-510, 1996.

[4] J.P. Hathout, A.M. Annaswamy, M. Fleifil, and A.F. Ghoniem. "A Model-based Active Control Design for Thermoacoustic Instability," *Combustion Science and Technology*, Vol. 132, pp. 99-138, February 1998.

[5] A..M. Annaswamy, M. Fleifil, J.W. Rumsey, R. Prasanth, J.P. Hathout, and A.F. Ghoniem, "Thermoacoustic Instability: Model-based Optimal Control Designs and Experimental Validation," *IEEE Transactions on Control Systems Technology*, Vol. 8, No. 6, November 2000.

[6] P. Mehta, A. Banaszuk, M. Soteriou and I. Mezic, "Fuel Control of a Ducted Bluffbody Flame," *42nd Conference on Decision and Control*, Maui, Hawaii, December 2003.

[7] G.A. Richards, G. J. Morris, D. W. Shaw, S. A. Keeley and M. J. Welter, "Thermal Pulse Combustion," *Combustion Science and Technology*, Vol. 94, pp.57-85, 1993.

[8] T. Lieuwen, Y. Neumeier and B. T. Zinn, "The Role of Unmixedness and Chemical Kinetics in Driving Combustion Instabilities in Lean Premixed Combustors," *Combustion Science and Technology*, Vol. 135, pp.193-211, 1998.

[9] S. Park, A.M. Annaswamy and A.F. Ghoniem, "Heat Release Dynamics Modeling of Kinetically Controlled Burning," *Combustion and Flame*, Vol.128, pp.217-231, 2002.

[10] S. Park, A. M. Annaswamy and A. F. Ghoniem, "A Model-Based Self-tuning Controller for Kinetically Controlled Combustion Instability," *American Control Conference*, Anchorage, Alaska, USA, May 8-10, 2002.

[11] S. Evesque, A.P. Dowling, and A.M. Annaswamy, "Self-tuning Regulators for Combustion Oscillations," *Royal Society Journal Proceedings of the Mathematical, Physical and Engineering Sciences*, Vol. 459, Issue 2035, pp 1709-1749, 2003.

[12] A.J. Riley, S. Park, A.P. Dowling, S. Evesque, and A.M. Annaswamy, "Adaptive Closed-Loop Control on an Atmospheric Gaseous Lean-Premixed Combustor," *ASME Journal of Engineering for Gas Turbines and Power, (to appear), 2004*.

[13] B.J Brunell. "A System Identification Approach to Active Control of Thermoacoustic Instability," M.S. Thesis, Department of Mechanical Engineering, MIT, 2000.

[14] S. Murugappan, S. Park, A.M. Annaswamy, A.F. Ghoniem, S. Acharya, and D.C. Allgood, "Optimal Control of a Swirl Stabilized Spray Combustor Using System Identification Approach", *Combustion Science and Technology* , Vol.175, pp.55-81, 2003.

[15] Y. Neumeier, N. Markopoulos and B.T. Zinn, "A Procedure for Real-time Mode Decomposition, Observation and Prediction for Active Control of Combustion Instabilities," *In Proceedings of the IEEE Conference on Control Applications*, paper No. 97318, Hartford, CT, 1997.

[16] A. Banaszuk, Y. Zhang, and C. A. Jacobson. "Adaptive Control of Combustion Instability Using Extremum-seeking," *American Control Conference*, Chicago, IL, 2000.

[17] J. M. Cohen and T. J. Anderson, "Experimental Investigation of Near-blowout Instabilities in a Lean Premixed Step Combustor," AIAA 96-0819, *34th Aerospace Sciences Meeting and Exhibit*, 1996.

[18] C. O. Paschereit, W. Weisenstein and E. Gutmark, "Role of Coherent Structures in Acoustic Combustion Control," *AIAA 98-2433, 29th AIAA Fluid Dynamics Conference*, 1998.

[19] A. Wachsman, S. Park, A. M. Annaswamy and A. F. Ghoniem, "Experimental Verification of Model Based Control Strategies Using a Backward Facing Step Combustor," *International Colloquium on Combustion and Noise Control*, Cranfield University, Cranfield, UK, Aug 2003.

[20] J. G. Lee, K. Kim, and D. A. Santavicca, "Measurement of Equivalence Ratio Fluctuations and Its Effect on Heat Release During Unstable Combustion," *Proceedings of the Combustion Institute*, Vol. 28, 2000.

[21] J. M. Cohen, J. H. Stufflebeam, and W. Proscia, "The Effect of Fuel/Air Mixing on Actuation Authority in an Active Combustion Instability Control System," 2000-GT-0083 *Proceedings of ASME TURBOEXPO 2000, Munich*, Germany, May, 2000.

[22] J. Brouwer, B. A. Ault, J. E. Bobrow, and G. S. Samuelsen, "Active Control For Gas Turbine Combustors," *Proceedings of the Combustion Institute*, Vol. 23, pp. 1087-1092, 1990.

[23] F.E.C. Culick, "Combustion Instabilities in Liquid-Fueled Propulsion Systems (An Overview), AGARD Conference Proceedings, paper 1, 450, *The 72nd Propulsion and Energetics Panel Specialists Meeting*, 1988.

[24] J.P. Hathout, M. Fleifil, A.M. Annaswamy, and A.F. Ghoniem, "Combustion Instability and Active Control Using Periodic Fuel Injection," *AIAA Journal of Propulsion and Power*, Vol. 18, no. 2, pp.390 -399, March-April 2002.

[25] H. Najm and A. F. Ghoniem, "Modeling Pulsating Combustion Due to Flow-Flame Interactions in Vortex-Stabilized Pre-Mixed Flames," *Combustion Science and Technology*, Vol. 94, pp.259-278, 1993.

[26] P. Holmes, J. Lumley and G. Berkooz. Turbulence, Coherent Structures, Dynamical Systems and Symmetry, Cambridge University Press, 1996.